IEEE Access
Multidisciplinary | Rapid Review | Open Access Journal

Received February 12, 2019, accepted February 23, 2019, date of publication March 8, 2019, date of current version March 25, 2019.

Digital Object Identifier 10.1109/ACCESS.2019.2902311

A Novel Low-Crosstalk Driveline Based on Spoof Surface Plasmon Polaritons

SHUMIN ZHAO[1,2,3], HAO CHI ZHANG[4], (Member, IEEE), LIANGLIANG LIU[5], (Member, IEEE), JIAHAO ZHAO[1,2,6], AND CHENG YANG[7], (Member, IEEE)

[1]Department of Precision Instrument, Tsinghua University, Beijing 100084, China
[2]State Key Laboratory of Precision Measurement Technology and Instruments, Tsinghua University, Beijing 100084, China
[3]Luoyang Optoelectro Technology Development Center, Luoyang 471009, China
[4]School of Electrical and Electronic Engineering, Nanyang Technological University, Singapore 639798
[5]Research Center of Applied Electromagnetics, School of Electronic and Information Engineering, Nanjing University of Information Science and Technology, Nanjing 210044, China
[6]Beijing Innovation Center for Future Chip, Tsinghua University, Beijing 100084, China
[7]State Key Laboratory of Millimeter Waves, Southeast University, Nanjing 210096, China

Corresponding author: Jiahao Zhao (falxon@mail.tsinghua.edu.cn)

This work was supported in part by the National Natural Science Foundation of China under Grant 61774096, Grant 61631007, Grant 61571117, Grant 61501112, Grant 61501117, Grant 61401089, and Grant 61701246, in part by the 111 Project under Grant 111-2-05, in part by the Scientific Research Foundation of Graduate School of Southeast University under Grant YBJJ1649, in part by the Natural Science Foundation of Jiangsu Higher Education Institutions of China under Grant 17KJB140014, and in part by the Priority Academic Program Development of Jiangsu Higher Education Institutions.

ABSTRACT The crosstalk suppression of multichannel coupled drivelines is studied for high-performance integration of micro-electro-mechanical system arrays. By using traditional drivelines, for example, microstrip lines, the distance between adjacent drivelines should be large enough to reduce the multichannel coupling effects. As a result, the size and the area of ultra-low crosstalk and closed-packaged driveline become an issue for design. To address it, we proposed a new scheme of multichannel spoof surface plasmon polaritons (SSPP)-based drivelines. The new drivelines consist of multiple parallel planar corrugated metallic strips. Thanks to the strong field confinement and localization characteristics of the SSPPs, the coupling effects between drivelines in different channels can be significantly suppressed with no need of any other coupling suppression circuits. For demonstration and investigation, both simulation and measurement are carried out up to 20 GHz. The results show that the crosstalk by using the proposed new drivelines can be reduced by about 10 dB on average. Therefore, the SSPP-based multichannel drivelines would be a good candidate for large-scale advanced integrated devices and systems with requirements of both miniaturization and coupling suppression.

INDEX TERMS Coupling suppression, driveline, low-crosstalk, spoof surface plasmon polaritons (SSPPs).

I. INTRODUCTION

The Micro-electro-mechanical system (MEMS) was proposed in the 1970s for the application of pressure/temperature sensors, accelerometers, gas chromatographs, as well as high-frequency switches and phase shifters [1]. Due to the requirement of small size for the MEMS, the room for drivelines is rather limited, and thus significant coupling effect appears between the drivelines and the signal lines, especially in the high-power applications. To avoid a mistaken switch-on led by the high average voltage of radio frequency (RF) signals, a threshold value for the drive-voltage is designed to be as high as 60 V [2], [3], which leads to high requirements in the mutual coupling suppression. Moreover, the strong mutual coupling between the adjacent drivelines induces a malop-eration of the adjacent MEMS and thus shortens the life of adjacent MEMS switches. More importantly, if the driveline is placed around an active chip, which is driven by a low voltage, the active chip will suffer from huge damages and malfunctions. In the traditional coupling suppression scheme, a lot of extra areas and spaces has to be reserved for transmission lines to suppress the high frequency multichannel signals, leading to a tradeoff between miniaturization and coupling suppression. Thus, the aforementioned contradictory is a research hotspot and has not been reported.

The associate editor coordinating the review of this manuscript and approving it for publication was Ildiko Peter.

Surface plasmon polariton (SPP) exists in nature at optical frequencies on the interface between one material with positive permittivity (e.g., dielectrics or vacuum) and another with negative permittivity (e.g. metals in this frequency regime) [4]. Due to permittivity discontinuity at the boundary, surface charges are deduced and surface waves propagate along the interface whist and decay exponentially in the transverse plane. Surface plasmon polariton possesses significant field enhancement and confinement, which are highly treasured in the development of compact communication devices and integrated systems. Unfortunately, natural SPPs vanish below infrared frequency as metals behave like perfect electric conductors (PEC) at low frequency [5].

Recently, a metamaterial approach of spoof surface plasmon polaritons (SSPPs) has been widely investigated at THz and microwave regimes [6]–[14] because it inherits the unique properties of optical SPPs, such as the significant field confinement and enhancement to overcome the diffraction limit. Therefore, corrugated metallic structures are engineered to reduce the plasmonic frequencies of metals to low frequencies. SSPPs also reserve advantages such as high confinement, low loss, and controllable dispersion properties [13]–[16]. It is demonstrated that double-strip SSPP-based transmission lines (TLs) can be tightly packed with deep-subwavelength separation to address the challenge of broadband signal integrity in modern integrated circuits. However, most driveline signals are pulsed, which have broadband spectra. Thus, for the MEMS applications, the suppression of mutual coupling should have a broadband behavior rather than only designed for specific working frequencies as [16].

In this work, we propose a new effective scheme of multichannel SSPPs-based TLs realized by multiple parallel planar corrugated metallic strips, to inhibit the mutual coupling effect between the multichannel drivelines in MEMS. Numerical and experimental results demonstrate that the mutual coupling effect between two SSPP-based TLs can be significant reduced without any other coupling suppression circuits, due to the strong field confinement and localization of the SSPPs. This indicates that the SSPP-based multichannel drivelines for MEMS arrays can be compatible with miniaturization and coupling suppression simultaneously in large-scale advanced integrated circuits and systems.

II. RESULTS

A. THE REQUEST OF THE RF MEMS PHASE SHIFTER ARRAY

The MEMS phase shifter constructed by MEMS switch array has the features of small insertion loss and low power consumption. It is necessary to construct a radiation-directional-reconfigurable antenna array with a series of MEMS phase shifter, which plays an important role in modern communication and radar systems. In an antenna array, the distance between adjacent phase shifters is about half of the wavelength of the center operation frequency, and a 3-bit MEMS phase shifter needs to include more than 3 MEMS switches. This implies that more than 3 drivelines should be included in an array in this near-half-wavelength space.

For time-sharing work communication system, system designers often want to increase the transmission power for a better communication coverage, which, however, introduces higher requirements for MEMS phase shifter arrays. In addition to the demand for the development of reliable high power MEMS switches for phase shifters, another important challenge is that the resulting crosstalk in MEMS switch drive line produces more serious problems: in order to avoid the self-pull phenomenon in MEMS switches when high-power signals are transmitted, high power MEMS switches with high driving voltage matching are required. Thus, MEMS phase shifter arrays contain many high power MEMS switches as well as a large number of corresponding high-voltage drive lines. In a compact communication system, these high-voltage drive lines have to be in line with conventional low-voltage signal lines with high density arrangement. These low-voltage signal lines mostly transmit low-voltage power supply signals / control signals, and are often connected to active devices that are vulnerable to short time high voltages. As such, the voltage jump on the high-voltage drive line will cause two technical risks that cannot be ignored: (1) A high coupling voltage may be generated on adjacent low-voltage signal lines, resulting in damages in the low-voltage resistance active devices or causing fluctuations in power supply / control signals; (2) A high coupling voltage can be generated on the high-voltage drive lines of adjacent MEMS switches, which may cause incorrect operation of those MEMS switches connected to the disturbed drive line, and may shorten the life cycle of those disturbed MEMS switches. Hence, in those systems, providing enough isolation between TLs is a very important issue. It is noteworthy that the difference between driveline systems and traditional signal systems is the signal voltage level. In order to drive MEMS switches, the operation voltage is over the 100 V. Hence, in order to avoid the breakdown of dielectric substrates (200 V each millimeter for Rogers RT 5880 used in this paper), it is necessary to optimize the thickness of the dielectric substrate. Here, we chose the thickest dielectric substrate type (the Rogers RT 5880 with a 1.575 mm-thick dielectric substrate). Moreover, for the MEMS array case, the distance between adjacent drivelines should be larger than 3 mm, because the voltage difference of adjacent drivelines may be amplified when they have the opposite phases. Hence, in our simulation and experiment, the smallest separation is set as 3 mm [17], [18].

B. THE FIELD CONFINEMENT TRANSMISSION LINE

In order to suppress the coupling between adjacent TLs, one of the potential schemes is to enhance the field confinement of the transmission line. Recently, SSPP transmission line is proposed to support the SPP-like mode, which has the feature of field enhancement and has been proved to be able to suppress the coupling in the frequency band of microwave [16], [19]–[22]. Though the SSPP TLs have

very good performance, as aforementioned, the separation between adjacent lines and the thickness of dielectric substrates should be carefully designed and chosen. Also, MEMS is driven by broadband signals in real applications, such as square wave signals. More importantly, the low-frequency components in such signals are always larger than the high-frequency components. Therefore, the existing design cannot be directly used in our case. Hence, our design and experiment are focused on a new kind of single-strip SPP transmission line.

As shown in Fig. 1(a), we designed a SSPPs-based multichannel TLs, which are composed of corrugated metallic strips printed on a dielectric substrate. The distance between two adjacent SPP transmission lines is designed to be equal to Dis, which is the distance between two microstrip (MS) lines and is shown in Fig. 1(b). Geometric parameters of the SSPP structure are denoted in Fig. 1(c) and Fig. 1(d) including the groove depth d, groove width a, strip thickness tm, period p, width w.

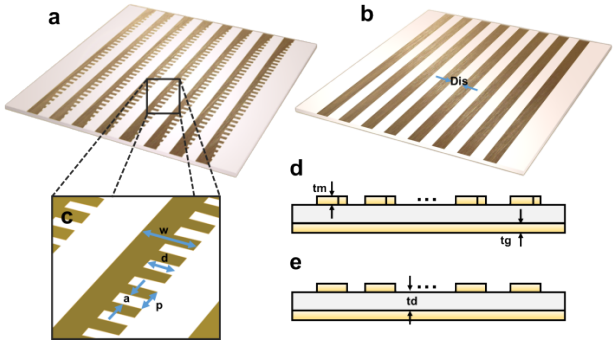

FIGURE 1. Schematic diagrams of SSPPs-based and microstrip drivelines. (a) The schematic diagram of the SSPPs-based driveline array structure. (b) The schematic diagram of the microstrip driveline array structure. (c) The enlarged view of the SSPPs-based driveline unit cell. (d) and (e) The lateral view of the SSPPs-based driveline (d) and microstrip (e) driveline array.

Such a plasmonic waveguide supports the surface wave mode with dispersion relation as

$$\sqrt{k_x^2 - k_0^2} = \alpha_T \tag{1}$$

where k_x and $k_0 = \omega/c$ are wave vectors along the propagation direction (x-direction here) and in free space, respectively. ω is the angular frequency of incident wave, and c is the velocity of the light line. α_T represents the decay constant along the tangential direction (y- or z- direction here). It is easy to understand that a larger k_x results in a higher α_T, indicating stronger field confinement and lower mutual coupling between neighboring TLs.

The dispersion diagrams of a microstrip line, a grounded single-strip SSPP-based transmission line and a non-grounded single-strip SSPP-based transmission line are shown in Fig. 2(a). Here, the period p = 3 mm, groove width a = 1.5 mm, groove depth d = 2.5 mm, width of the SSPP-based transmission line w = 5 mm (equal to the width of the SSPP-based transmission line) and the thicknesses of the metal strip and the ground tm = tg = 0.07 mm. The dielectric substrate with a thickness td = 1.575 mm is Rogers RT5880, whose relative permittivity ε_r is 2.2 and loss tangent tanδ is 0.0009. The dispersion curves were obtained through a full-wave simulation with the Eigen-mode solver carried out by the commercial software CST Microwave Studio. In this simulation, the loss of metals and dielectrics is ignored. According to a previous research [16], ignoring the loss would only produce a tiny blue shift on the dispersion spectrum and negligible influence on the shape of the dispersion curve, which, on the other hand, can greatly simplify the Eigen-mode simulation, and reduce the calculation time.

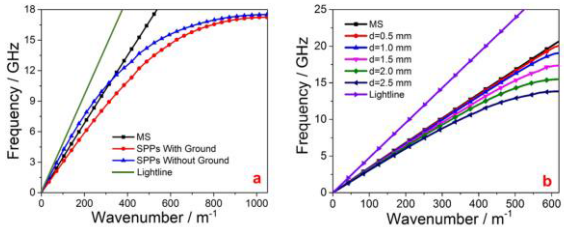

FIGURE 2. Dispersion curve diagrams of the SSPPs. (a) Dispersion curves of a microstrip line, a grounded and a non-grounded single-strip SSPP-based TLs in which p = 3 mm, a = 1.5 mm, d = 2.5 mm, w = 5 mm and tm = tg = 0.07 mm. (b) Dispersion curves of the grounded SSPPs unit with different groove depth d in which p = 3 mm, a = 1.5 mm, w = 5 mm and tm = tg = 0.07 mm.

It is observed that the dispersion curve of the non-grounded single-strip SSPP-based transmission line has a cross-point with that of the microstrip line. Below the frequency at the cross-point (fc), the non-grounded SSPP-based transmission line has a smaller wave number than that of the microstrip line, and therefore has lower transmission loss [15]. Above fc, the non-grounded SSPP-based transmission line has a larger wave number and therefore leads to lower mutual coupling [16]. In contrast, the dispersion curve of the grounded SSPP-based transmission line is always on the right of the microstrip line, indicating better performance in terms of mutual coupling in the whole pass-band. One of the most important advantages of the SSPPs is that its dispersion curve can be arbitrarily controlled by changing the geometrical parameters, which can be utilized to achieve wavenumber matching between two TLs. Here, we show this feature in Fig. 2(b). In our simulations, the parameters in Fig. 2(b) are chosen to be the same as that in Fig. 2(a) except the groove depth d, which varies from 0 to 2.5 mm with a step of 0.5 mm. In Fig. 2(b), we can clearly observe that, the dispersion curves of SSPP-based TLs with different groove depths gradually deviate from the light line and the microstrip line, as the frequency increases and then asymptotically approaches different cutoff frequencies, which is similar to natural SPPs and indicates stronger field confinement.

Next, we tested mutual coupling when the distances between eight grounded SSPP-based TLs and eight microstrip lines are reduced to sub-wavelength scale. The reason why we chose eight lines is that the design of 8 parallel

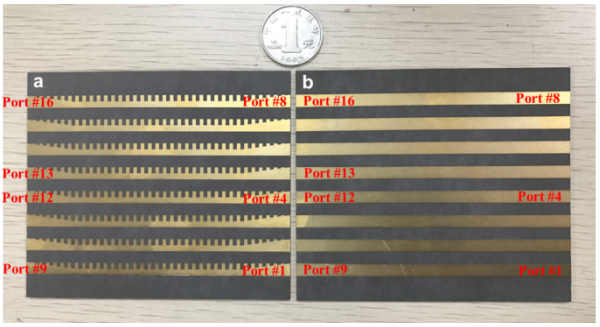

FIGURE 3. The photograph of the samples. (a) The SSPPs-based driveline array. (b) The microstrip driveline array.

drive lines is common for the real applications of MEMS antenna arrays.

Numerical simulation was conducted by the time domain solver of the commercial software of CST Microwave Studio, where 16 ports were defined, as shown in Fig. 3. Note that a conversion section, which is composed of gradient corrugated strips as presented in [23], is inserted between the SSPP-based transmission line and the feeding port for impedance and momentum matching. Meanwhile, based on the coupled mode theory [15], the transmitted power ratio (T) and the coupling power ratio (C) of adjacent waveguide systems can be expressed analytically as

$$\begin{aligned} T &= \cos^2(\kappa L)e^{-2\alpha L} \\ C &= \sin^2(\kappa L)e^{-2\alpha L} \end{aligned} \tag{2}$$

where L is the coupling length of the waveguide, α is the imaginary part of the propagation constant, and κ is the frequency-dependent coupling coefficient written as [15]

$$\kappa = \frac{\omega\varepsilon_0}{4}\iint (n^2 - n_0^2)\left[E_{1t}^* \cdot E_{2t} + \frac{n_0^2}{n^2}E_{1n}^* \cdot E_{2n}\right]dS \tag{3}$$

in which, n and n_0 are the refractive indices of the surrounding medium and the plasmonic waveguide, respectively. E_{jt} and E_{jn} ($j = 1, 2$) are the normalized transverse and longitudinal electric fields in TLs j, respectively. From (2), it is observed

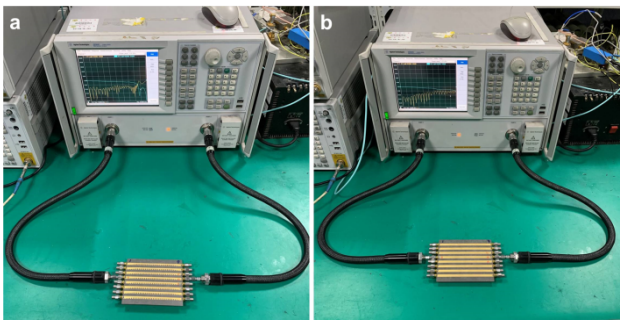

FIGURE 4. The photographs of the real test equipment (VNA, E8364C). (a) Testing the SSPPs-based driveline array. (b) Testing the microstrip driveline array.

that the coupling of TLs is caused by the overlap of the electric fields in two adjacent waveguides. Hence it is possible to suppress the crosstalk between two TLs using the excellent feature of field confinement of SSPPs. Meanwhile, since the strongest coupling occurs between adjacent TLs, without loss of generality, we only cared about the coupling power ratio from port 4 to port 13. In fact, it is noted that the far-end crosstalk becomes the main crosstalk in our case, because this case can be considered as weak coupling for distances larger than 3 mm. On the other hand, in a communication system, the near-end crosstalk affects the matched state of adjacent channels. However, in our drive line system, only the far-end signal form is important. Hence, we focus our experiment and simulation on the far-end crosstalk.

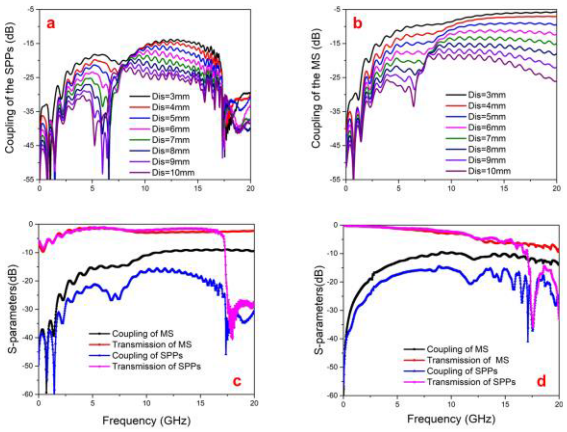

FIGURE 5. Simulated and experimental transmission and coupling frequency spectrum diagrams of the two samples. (a) The simulated result of coupling of the SSPPs structure with different widths of the gap Dis. (b) The simulated result of coupling of the MS structure with different widths of the gap Dis. (c) The simulated result of transmission and coupling of the SSPPs and MS structures. (d) The experimental result of transmission and coupling of the SSPPs and MS structures.

Fig. 5(a) and 5(b) clearly demonstrate that the mutual coupling between two SSPP-based TLs is much lower than that of the two microstrip lines, when the separation Dis varies in a sub-wavelength scale from 3 mm to 10 mm. Furthermore, the simulated and measured S-parameters are directly compared between these two kinds of TLs in Fig. 5(c) and (d), respectively. It is observed that the coupling coefficient of the SSPPs-based TLs maintains lower than that of the microstrip (MS) TLs, even though the separation is reduced to 3 mm (1/10 λ_0 at 10 GHz). In contrast, the transmission of the MS line decreases significantly with the same separation. Moreover, the figures also show that the coupling are comparable for these two kinds of TLs, and the SPP transmission line performs better at frequencies lower than the cut-off frequency. This figure, in addition, indicates that the modeling and configuration of multi-ports are reasonable.

Moreover, it is clear that the transmission and coupling of the adjacent drivelines are relative with the coupling length L. Hence, in order to verify the appropriation of our design, the simulated coupling frequency spectrum diagrams of the two samples with different coupling lengths are also investigated

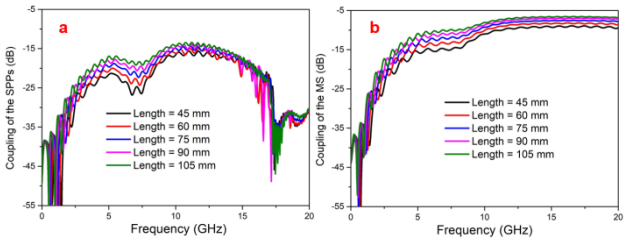

FIGURE 6. Simulated coupling frequency spectrum diagrams of the two samples with different coupling lengths. (a) The simulated result of coupling of the SSPPs structure with different coupling lengths. (b) The simulated result of coupling of the MS structure with different coupling lengths.

in Fig. 6. Form this figure, it is clear that the coupling of the SSPPs TLs is smaller than that of MS for all coupling lengths, which means that the SSPPs driveline can be applied to applications with different lengths.

In order to verify our work experimentally, we fabricated SSPPs-based and microstrip driveline arrays, as shown in Fig. 3. Meanwhile, the matching load and the coaxial line used in the experiment, and the parameters of these two samples are the same as those of the above simulation model. The separation is chosen as 5 mm, considering the width of SMA connectors.

In the experiment, an Agilent vector network analyzer (VNA, E8364C) was used to obtain the reflection, transmission and coupling coefficients of the samples. In order to connect drivelines with the VNA, 16 standard SMA connectors are used to connect the 16 ports of the sample. The photographs of the real testing equipment (VNA, E8364C) are illustrated in Fig. 4 .The measured transmission and coupling coefficients of the two kinds of drive lines are illustrated in Fig. 5(d), which are in good agreement with the simulation results. Due to the fact that the system is linear, we were able to measure the transmission, reflection and coupling of different ports in turn. In the measurement, the extra ports are connected to matching loads to minimize the effect of them. In Fig. 5(d), it is clearly observed that the coupling between the SSPPs-based TLs is about 10 dB smaller than that of the microstrip lines from 5 GHz to 15 GHz, which implies that the coupling between microstrip TLs is 10 times stronger than that of SSPPs TLs. Meanwhile, the transmission coefficients of the SSPPs-based TLs and the microstrip TLs are almost the same in the whole passband. The transmission capabilities of the microstrip TLs and the SSPPs TLs are both weaker than the simulated results, which may result from the extra loss of the dielectric substrate, the connectors or the welding discontinuity. On the other hand, the difference at the lower frequency maybe caused by the convergence precision of the time domain solver of the CST microwave studio. In a word, the simultaneous difference between the simulation and experiment for both MS and spoof SPP TLs does not affect the qualitative conclusion on the effect of coupling suppression because the performance deterioration is mainly led by some general causes rather than properties of the kind of TLs.

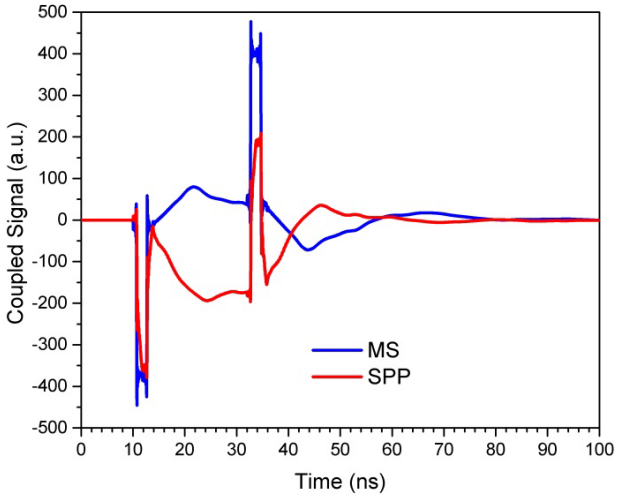

FIGURE 7. The coupling time domain signal of different samples.

Finally, to show a visualized result, we measured the output transmission and the coupling time domain signals, as shown in Fig. 7. In this case, the input signal was set as a step signal with a 2 ns rising edge, and the total input power was set as 1 W. Here, the reason why we did not set the voltage is that the voltage was affected by the reflection wave in the driveline. In this figure, it is clearly observed that, the peak of the coupling signal level can be significantly reduced in the SSPPs-based TLs, compared to that in the microstrip TLs, which implies that the proposed SSPPs-based structure can reduce the peak coupling voltage level of MEMS to avoid incorrect operation.

III. CONCLUSION

In this paper, we have presented a significantly improved scheme for mutual coupling suppression by a grounded single-strip SSPP-based transmission line. Simulated and experimental results indicate that the mutual coupling effect between two SSPP-based TLs can be significant reduced without any other coupling suppression circuits, thanks to the strong field confinement and localization of the SSPPs. Hence, we may have a potential solution to the signal crosstalk in compact circuits. Moreover, the proposed SSPPs-based TLs are suitable for the driveline of the MEMS switch array, because they are able to suppress the coupling to avoid damages and distortion in switches.

REFERENCES

[1] G. M. Rebeiz, *RF MEMS: Theory, Design, and Technology*. Hoboken, NJ, USA: Wiley, 2003.
[2] C. D. Patel and G. M. Rebeiz, "A high-reliability high-linearity high-power RF MEMS metal-contact switch for DC–40-GHz applications," *IEEE Trans. Microw. Theory Techn.*, vol. 60, no. 10, pp. 3096–3112, Oct. 2012.
[3] H.-H. Yang, H. Zareie, and G. M. Rebeiz, "A high power stress-gradient resilient RF MEMS capacitive switch," *J. Microelectromech. Syst.*, vol. 24, no. 3, pp. 599–607, Jul. 2015.
[4] W. L. Barnes, A. Dereux, and T. W. Ebbesen, "Surface plasmon subwavelength optics," *Nature*, vol. 424, no. 6950, pp. 824–830, 2003.
[5] S. A. Maier, *Plasmonics: Fundamentals and Applications*. New York, NY, USA: Springer, 2007.

[6] J. B. Pendry, L. Martín-Moreno, and F. J. Garcia-Vidal, "Mimicking surface plasmons with structured surfaces," *Science*, vol. 305, pp. 847–848, Aug. 2004.
[7] A. P. Hibbins, B. R. Evans, and J. R. Sambles, "Experimental verification of designer surface plasmons," *Science*, vol. 308, no. 5722, pp. 670–672, Apr. 2005.
[8] F. J. Garcia-Vidal, L. Martín-Moreno, and J. B. Pendry, "Surfaces with holes in them: New plasmonic metamaterials," *J. Opt. A, Pure Appl. Opt.*, vol. 7, no. 2, p. S97, 2005.
[9] S. A. Maier, S. R. Andrews, L. Martín-Moreno, and F. J. García-Vidal, "Terahertz surface plasmon-polariton propagation and focusing on periodically corrugated metal wires," *Phys. Rev. Lett.*, vol. 97, pp. 176805-1–176805-4, Oct. 2006.
[10] N. Prashant, C. L. Nathan, O. Sang-Hyun, and J. N. David, "Ultrasmooth patterned metals for plasmonics and metamaterials," *Science*, vol. 325, no. 5940, pp. 594–597, Jul. 2009.
[11] X. Shen, T. J. Cui, D. F. Martin-Cano, and J. Garcia-Vidal, "Conformal surface plasmons propagating on ultrathin and flexible films," *Proc. Nat. Acad. Sci. USA*, vol. 110, no. 1, pp. 40–45, Jan. 2013.
[12] H. F. Ma *et al.*, "Broadband and high-efficiency conversion from guided waves to spoof surface plasmon polaritons," *Laser Photon. Rev.*, vol. 8, pp. 146–151, Jan. 2014.
[13] L. Liu *et al.*, "Multi-channel composite spoof surface plasmon polaritons propagating along periodically corrugated metallic thin films," *J. Appl. Phys.*, vol. 116, Jun. 2014, Art. no. 013501.
[14] W. Sun, Q. He, S. Sun, and L. Zhou, "High-efficiency surface plasmon meta-couplers: Concept and microwave-regime realizations," *Light-Sci. Appl.*, vol. 5, p. e16003, 2016.
[15] H. C. Zhang *et al.*, "Smaller-loss planar SPP transmission line than conventional microstrip in microwave frequencies," *Sci. Rep.*, vol. 6, Mar. 2016, Art. no. 23396.
[16] H. C. Zhang, T. J. Cui, Q. Zhang, Y. Fan, and X. Fu, "Breaking the challenge of signal integrity using time-domain spoof surface plasmon polaritons," *ACS Photon.*, vol. 2, no. 9, pp. 1333–1340, Aug. 2015.
[17] Z. Y. Qian, "The analysis of Microstrip transmission line," (in Chinese), *J. Anhui Vocational College Electron., Inf. Technol.*, vol. 11, no. 4, pp. 36–39, 2012.
[18] Y. M. Feng, Q. Zhang, and K. S. Zhou, "The study of the relationship between air humidity and air breakdown field strength by using electrostatic gun," (in Chinese), *Technol. Life*, vol. 2, no. 15, pp. 20–21, 2010.
[19] D. J. Hou *et al.*, "Experimental measure of transmission characteristics of low-frequency surface plasmon polaritons in frequency and time domains," *Opt. Express*, vol. 24, no. 7, pp. 7387–7397, 2016.
[20] J. J. Wu *et al.*, "Differential microstrip lines with reduced crosstalk and common mode effect based on spoof surface plasmon polaritons," *Opt. Express*, vol. 22, no. 22, pp. 26777–26787, 2014.
[21] S. Bahrami and S. Fallahzadeh, "Near end crosstalk reduction using slow wave structures," *J. Electromagn. Waves Appl.*, vol. 30, no. 12, pp. 1566–1573, 2016.
[22] A. Kianinejad, Z. N. Chen, and C.-W. Qiu, "Low-loss spoof surface plasmon slow-wave transmission lines with compact transition and high isolation," *IEEE Trans. Microw., Techn.*, vol. 64, no. 10, pp. 3078–3086, Oct. 2016.
[23] W. Zhang *et al.*, "Trapping of surface plasmon wave through gradient corrugated strip with underlayer ground and manipulating its propagation," *Appl. Phys. Lett.*, vol. 106, Dec. 2015, Art. no. 021104.

SHUMIN ZHAO received the M.S. degree in navigation, guidance and control from Chinese Aeronautical Establishment, Beijing, China, in 2002. From 2002 to 2012, he was an Engineer with the Luoyang Optoelectro Technology Development Center, Luoyang, China. He is currently pursuing the Ph.D. degree in instrument science and technology with the Department of Precision Instrument, Tsinghua University, Beijing. He is also a member of the State Key Laboratory of Precision Measurement Technology and Instruments. His research interests include RF MEMS technology, microwave systems, and metamaterial technology.

HAO CHI ZHANG (S'15–M'18) was born in Jiaxing, Zhejiang, China, in 1991. He received the B.Eng. degree in electrical engineering from the University of Electronic Science and Technology of China, Chengdu, China, in 2013. He is currently pursuing the Ph.D. degree in electromagnetic and microwave technology from Southeast University, Nanjing, China. He is also with the School of Electrical and Electronic Engineering, Nanyang Technological University, Singapore, as a Project Officer. His current research interests include microwave and millimeter-wave circuits and antennas technology, surface plasmons, and metamaterials. He has authored over 30 international refereed journal papers, in highly ranked journals, including *Laser and Photonics Reviews*, *ACS Photonics*, the IEEE TRANSACTIONS ON ANTENNA AND PROPAGATION, and *Applied Physics Letters*.

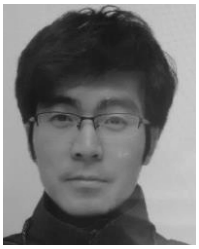

LIANGLIANG LIU was born in Jiangsu, China, in 1987. He received the B.S. degree in information engineering, the M.E. degree in electromagnetic field and microwave technology, and the Ph.D. degree in commutation and information system from the Nanjing University of Aeronautics and Astronautics, China, in 2010, 2013, and 2017, respectively. Since 2017, he has been an Associate Professor with the School of Electronic and Information Engineering, Nanjing University of Information Science and Technology. He has authored or co-authored over 40 papers in international refereed journals and conference proceedings. His current research interests include spoof surface plasmon polaritons, spoof localized surface plasmons, and metasurfaces.

JIAHAO ZHAO received the B.S. and Ph.D. degrees from the School of Materials Science and Engineering, Tsinghua University, Beijing, China, in 2000 and 2006, respectively.

From 2007 to 2010, he was a Postdoctoral Researcher with the Department of Precision Instrument and Mechanology, Tsinghua University, where he is currently an Associate Professor. His current research interests include RF-MEMS and space MEMS technology.

CHENG YANG (M'17) received the B.S. degree in electronic science and technology from Wuhan University, Wuhan, China, in 2009, and the M.S. and Ph.D. degrees in electromagnetic field and microwave technology from the National University of Defense Technology, Changsha, China, in 2012 and 2016, respectively.

From 2013 to 2015, he has been funded by the Chinese Scholarship Council for a joint research at the Institute of Electromagnetic Theory, Hamburg University of Technology, Germany. Since 2017, he has been a Faculty Member with the State Key Laboratory of Millimeter Wave, Southeast University, China. His current research interests include numerical techniques in electromagnetics, calibration techniques in microwave measurements, and scattering and propagation studies of nonlinear metamaterials.